Singularity Issues in Fixture Fault Diagnosis for Multi-Station Assembly Processes

Yu Ding

Abhishek Gupta

Department of Industrial Engineering,
Texas A&M University, TAMU 3131
College Station, TX 77843-3131

Daniel W. Apley

Department of Industrial Engineering and
Management Sciences,
Northwestern University,
Evanston, IL 60208-3119

This paper presents a method of diagnosing variance components of process error sources in singular manufacturing systems. The singularity problem is studied and the cause examined in the context of fixture error diagnosis in multi-station assembly processes. The singularity problem results in nondiagnosable fixture errors when standard least-squares (LS) estimation methods are used. This paper suggests a reformulation of the original error propagation model into a covariance relation. The LS criterion is then applied directly to the sample covariance matrix to estimate the variance components. Diagnosability conditions for this variance LS estimator are derived, and it is demonstrated that certain singular systems that are not diagnosable using traditional LS methods become diagnosable with the variance LS estimator. Modified versions that improve the accuracy of the variance LS estimator are also presented. The various procedures are thoroughly contrasted, in terms of accuracy and diagnosability. The results are illustrated with examples from panel assembly, although the application of the approach and the conclusions extend to more general discrete-part manufacturing processes where fixtures are used to ensure dimensional accuracy of the final product. [DOI: 10.1115/1.1644549]

1 Introduction

Dimensional variation is a major problem affecting product quality in discrete-part manufacturing. In automotive and aerospace industries, for example, dimensional problems contribute to roughly two-thirds of all quality-related problems during new product launch [1,2]. Dimensional quality of the finished product in panel assembly depends largely on the accuracy of the fixtures used to hold parts. Fixture locators are used extensively in multi-station assembly processes, such as automotive body assembly and aircraft fuselage assembly, in order to provide part support and dimensional reference within a given coordinate system, thereby determining the dimensional accuracy of the final assembly [2,3]. Fixture locators may fail to provide the desired positioning repeatability (relative to tolerances) during production due to gradual deterioration of locators and/or catastrophic events such as broken locators. Considerable efforts have been made in recent years to diagnose fixture errors (sometimes referred to as ''fixture faults'') based on product dimensional measurements [4–10]. In these works, the effects of fixture errors on dimensional measurements are represented via the linear diagnostic model

$$\mathbf{y}(t)=\mathbf{D}\mathbf{u}(t)+\mathbf{v}(t), \quad t=1,\ldots,M, \tag{1}$$

where $\mathbf{y}(t)$ is the vector of n measured product features, $\mathbf{u}(t)$ is the vector of p error sources, $\mathbf{v}(t)$ is the additive noise vector (e.g., sensor noise), $\mathbf{D}=[\mathbf{d}_1,\mathbf{d}_2\ldots,\mathbf{d}_p]$ is an $n\times p$ diagnostic matrix linking fixture errors to measurements, t is the observation number index, and M is the sample size. Elements in $\mathbf{u}(t)$ are assumed independent random variables because fixture locators are assumed physically independent. It is normally assumed that the sensor system is such that the elements of the noise vector are independent and have equal variance σ_v^2. Thus, the covariance matrix of $\mathbf{v}(t)$ is $\sigma_v^2\mathbf{I}$. The matrix $\mathbf{D}$ can be determined from the relative positions of fixture locators and sensors using standard kinematics analyses [4–9]. Fixture errors manifest themselves as mean shifts and variance in the elements of $\mathbf{u}(t)$. Diagnosing fixture errors is equivalent to estimating the mean and variance components of $\mathbf{u}(t)$ based on the sample of measurement observations $\{\mathbf{y}(t)\}_{t=1}^M$. The focus of this paper is diagnosis of fixture error *variance components*, as opposed to mean shifts.

Most approaches are based on least-squares (LS) estimation, with a typical procedure as follows. The following procedure has been slightly modified to accommodate a nonzero mean in $\mathbf{y}$ (for the original presentation of this procedure, please refer to, e.g., Apley and Shi [5]): (DP1) Estimate $\hat{\mathbf{u}}(t)=(\mathbf{D}^T\mathbf{D})^{-1}\mathbf{D}^T(\mathbf{y}(t)-\overline{\mathbf{y}})$, where the sample mean $\overline{\mathbf{y}}=(\Sigma_{t=1}^M\mathbf{y}(t))/M$; (DP2) Estimate $\hat{\sigma}_v^2=(1/(M-1)(n-p))\Sigma_{t=1}^M\hat{\mathbf{v}}(t)^T\hat{\mathbf{v}}(t)$, where $\hat{\mathbf{v}}(t)=\mathbf{y}(t)-\overline{\mathbf{y}}-\mathbf{D}\hat{\mathbf{u}}(t)$; (DP3) Estimate the variance components of $\mathbf{u}$: $\hat{\sigma}_i^2=(1/(M-1)\Sigma_{t=1}^M\hat{u}_i(t)^2-\hat{\sigma}_v^2(\mathbf{D}^T\mathbf{D})_{i,i}^{-1}$, where $\hat{u}_i(t)$ represents the ith element of $\hat{\mathbf{u}}(t)$ and $(\mathbf{D}^T\mathbf{D})_{i,i}^{-1}$ is the (i,i)th element of $(\mathbf{D}^T\mathbf{D})^{-1}$.

The interpretation is that we first estimate the random deviations $\{\hat{\mathbf{u}}(t)\}_{t=1}^M$, and then use the sample variance of their elements to estimate the variance components of $\mathbf{u}$. The quantity $\hat{\sigma}_v^2(\mathbf{D}^T\mathbf{D})_{i,i}^{-1}$ is subtracted out in order to eliminate bias due to measurement noise. Because the deviations $\{\hat{\mathbf{u}}(t)\}_{t=1}^M$ are directly estimated via LS, this estimator will be referred to as a ''deviation LS estimator.''

In order to implement procedure (DP1) to (DP3) and produce unique estimates, the following conditions are required: i) $\mathbf{D}^T\mathbf{D}$ must be of full rank, or equivalently, the columns of $\mathbf{D}$ must be linearly independent; and ii) $n>p$. These conditions are often satisfied for simple single-station assembly processes when a sufficient number of sensors are used to measure all degrees of freedom of each workpiece. System singularity ($\mathbf{D}^T\mathbf{D}$ singular) is often encountered in complex multi-station assembly processes, however, where sensors can only be placed at a downstream station but variation sources are contributed from upstream stations. Singularity is also common in compliant-part assembly processes, where there are modes of rigid-body motion and compliant-part deformation [11]. Section 2 provides an example of singularity in multi-station assembly.

LS modifications using generalized inverses and singular value decomposition [12,13] and partial least squares [14] have been

Contributed by the Manufacturing Engineering Division for publication in the JOURNAL OF MANUFACTURING SCIENCE AND ENGINEERING. Manuscript received Feb. 2003. Associate Editor: S. Jack Hu.

 Copyright © 2004 by ASME

developed to accommodate singularity and ill-conditioning in parameter estimation [15,16]. The basic idea behind these approaches is to transform the columns of **D** into a smaller set of linearly independent basis vectors that span the column space of **D**, and then use LS on the reduced-dimenaionality problem. Although these are appropriate for many parameter estimation problems, they may lead to erroneous conclusions in fixture diagnosis. The reason is that because the columns of **D** and the associated variance components represent actual physical phenomena, any reduction in dimensionality and transformation of the columns of **D** will void its physical meaning. Rong et al. [11] proposed a partial solution to this problem that they termed adjusted least squares. They partitioned $\mathbf{D}=[\mathbf{D}_1|\mathbf{D}_2]$, where $\mathbf{D}_1$ consists of the columns of **D** that are linearly independent of all other columns. In other words, for any linear combination $\alpha_1\mathbf{d}_1+\alpha_2\mathbf{d}_2+\ldots+\alpha_p\mathbf{d}_p$ that equals zero, the coefficients associated with the columns of $\mathbf{D}_1$ must be zero. Assuming the set of linearly independent columns is nonempty, their method will provide a unique estimate of the subset of variance components associated with the columns of $\mathbf{D}_1$. As in standard least squares, the estimates of the other variance components (associated with the columns of $\mathbf{D}_2$) are nonunique.

This paper presents an approach that can provide unique estimates of all variance components in situations that satisfy certain diagnosability conditions, even if $\mathbf{D}^T\mathbf{D}$ is singular. We demonstrate that the deviation LS estimator ignores important information that can be utilized for this purpose and derive a diagnosability condition for the new estimator that is more relaxed than the diagnosability condition for the deviation LS estimator. The relationships between the various estimators are thoroughly discussed.

The format of the remainder of the paper is as follows. Section 2 reviews the modeling procedure for fixture error propagation and explains the cause of singularity in multi-station models. Section 3 introduces a new variance estimator and two modifications that improve performance. Section 3 also derives the diagnosability condition for the new estimator. Section 4 presents several examples of multi-station assembly processes corresponding to the situations discussed in Section 3. Section 5 concludes the paper.

2 A Variation Model and Singularity in Multi-Station Processes

Previous work has developed a fixture-error propagation model for general multi-station discrete-part manufacturing systems such as rigid-part assembly processes [17–19], compliant-part assembly processes [20], and machining processes [21,22]. In this section, we use a simplified two-station panel assembly process to illustrate the modeling procedure, and explain the cause of system singularity. Details on the modeling procedure can be found in Jin and Shi [17] and Ding et al. [18].

Fixtures in multi-station panel assembly processes generally use an n-2-1 layout, consisting of two locating pins and n NC blocks to determine the part/subassembly location and orientation. A typical 3-2-1 (i.e., $n=3$) fixture is shown in Fig. 1. The two locating pins, P_{4way} and P_{2way}, constrain the three degrees of freedom of a part in the X-Z plane, where the 4-way pin restricts part motion in both the X- and Z-directions, and the 2-way pin restricts part motion in the Z-direction. The three NC blocks, NC_i, $i=1, 2, 3$, constrain the remaining degrees of freedom of the workpiece in the Y-direction. When a workpiece is non-rigid, more than three NC blocks may be needed in order to reduce part deformation. For simplicity, this section illustrates with a 2D example in the X-Z plane (in which the part is rigid). More general modeling examples that result in the same linear model structure of Eq. (1) can be found in the aforementioned literature [17–22].

In a multi-station process, 3-2-1 fixtures are repeatedly used at every station to support parts/subassemblies. To illustrate, we refer to the following example throughout the paper. Figure 2 shows a two-station process, which is a segment of the simplified automotive body assembly process from [10]. Three workpieces are welded together at Station I. The first workpiece consists of two components and is a subassembly from the preceding assembly operation. After the welding operation is finished, the whole assembly is transferred to a dedicated measurement station (Station II) for inspection. This simple two-station segment involves all necessary assembly process operations, including positioning, joining, transferring, and inspection. A full-scale assembly process will simply repeat these operations when fabricating complex products.

In this process, each part or subassembly (consisting of several parts) is restrained by a 3-2-1 fixture. Locators being used are marked P_1-P_6 in Fig. 2 (note that P_1 and P_6 are used to position the whole subassembly in Station II). NC blocks are not shown since we are considering a 2D assembly process. The deviations of a 4-way locator in two directions or the deviation of a 2-way locator in the Z-direction could cause part deviation. They constitute 12 potential fixture errors, numbered 1–9 on Station I and 10–12 on Station II, with arrows indicating their deviation directions.

In such a 2D multi-station process, each part has three degrees of freedom. We use $\mathbf{x}_{i,k}$ to denote the deviation state of part i at station k,

$$\mathbf{x}_{i,k}=[\,\delta X_{i,k}\quad \delta Z_{i,k}\quad \delta\alpha_{i,k}]^T, \tag{2}$$

where δ is the perturbation operator and α is the orientation angle. Thus the state of the product, which consists of n_p ($n_p=4$ in this process) parts, is represented by

$$\mathbf{x}_k\equiv[\,\mathbf{x}_{1,k}^T\quad\cdots\quad\mathbf{x}_{n_p,k}^T]^T, \tag{3}$$

where $\mathbf{x}_{i,k}=\mathbf{0}$ if part i has not yet appeared at station k.

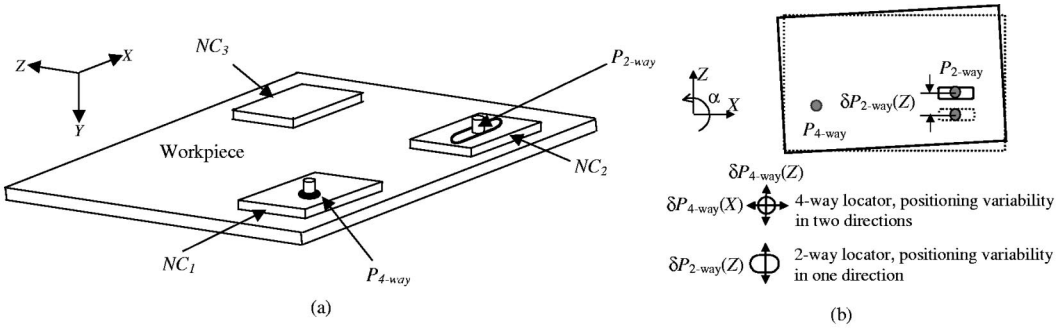

Fig. 1 Illustration of a 3-2-1 fixture

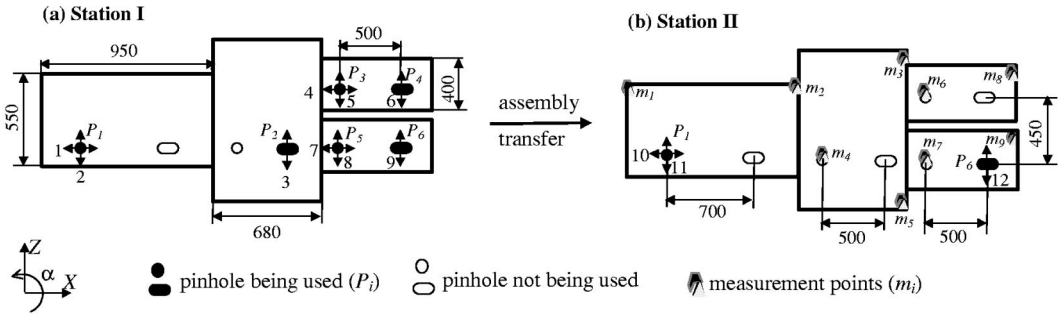

Fig. 2 A two-station assembly process (units in mm)

Random fixture errors on station k are represented by $\mathbf{u}_k$. Thus, we have $\mathbf{u}_1=[\delta p_1 \cdots \delta p_9]^T$, and $\mathbf{u}_2=[\delta p_{10}\ \delta p_{11}\ \delta p_{12}]^T$, where δp_j is the deviation associated with fixture error j.

Nine coordinate sensors, denoted by m_1 through m_9 in Fig. 2(b), are installed in Station II. Each coordinate sensor measures the position of a part feature (e.g. a corner or hole) in two orthogonal directions (X and Z), so that the total number of measurements is $n=18$. We use $\mathbf{y}$ to represent the positional deviations detected by sensors at product features. In the above process, since sensors are only available at Station II, we have $\mathbf{y}_1=\mathbf{0}$ and $\mathbf{y}_2=[\delta m_1(X)\ \delta m_1(Z) \cdots \delta m_9(X)\ \delta m_9(Z)]^T$, where $\delta m_j(X\ or\ Z)$ is the deviation detected at product feature j in the $X(or\ Z)$ direction.

For the two-station assembly process shown in Fig. 2, the state-space representation [10] of the fixture error propagation model becomes

$$\begin{aligned}\mathbf{x}_1&=\mathbf{A}_0\mathbf{x}_0+\mathbf{B}_1\mathbf{u}_1+\mathbf{w}_1\\ \mathbf{x}_2&=\mathbf{A}_1\mathbf{x}_1+\mathbf{B}_2\mathbf{u}_2+\mathbf{w}_2\\ \mathbf{y}_2&=\mathbf{C}_2\mathbf{x}_2+\mathbf{v}_2\end{aligned} \tag{4}$$

where $\mathbf{x}_0$ represents the part deviations resulting from the stamping process prior to the assembly process, $\mathbf{A}_1\mathbf{x}_1$ represents the transformation of the product dimensional deviation from Station I to Station II, $\mathbf{B}_k\mathbf{u}_k$ represents the product deviations resulting from process variations at station k ($k=1,2$), $\mathbf{C}_2$ characterizes the information regarding sensor locations at Station II, and $\mathbf{w}_k$ ($k=1,2$) represents the higher order terms and other un-modeled process errors. Detailed expressions for the **A**, **B**, and **C** matrices in the above equation can be found in [10] and will not be repeated here. The numerical expression for $\mathbf{A}_1$, which is needed in subsequent analyses, is provided in Appendix A1.

In the aforementioned literature [17–22] on the multi-station error propagation model, the state space representation is commonly adopted to model full-scale assembly and machining processes. Given a general N-station system as shown in Fig. 3, the state space variation model takes the form

$$\begin{aligned}\mathbf{x}_k&=\mathbf{A}_{k-1}\mathbf{x}_{k-1}+\mathbf{B}_k\mathbf{u}_k+\mathbf{w}_k \quad \text{and}\\ \mathbf{y}_k&=\mathbf{C}_k\mathbf{x}_k+\mathbf{v}_k, \quad k=1,\ldots,N\end{aligned} \tag{5}$$

where the notation corresponds to that in Eq. (4). Note that the subscript represents the station index and the observation index t is not explicitly included. Matrices $\mathbf{A}_k$, $\mathbf{B}_k$, and $\mathbf{C}_k$ are determined by process design and sensor deployment and $\mathbf{C}_k=\mathbf{0}$ if no sensor is installed at station k (e.g., $\mathbf{C}_1=\mathbf{0}$ in the above example). The first equation in (5) is called the *state transition equation* and $\mathbf{A}_{k-1}$ is accordingly called the *state transition matrix* because $\mathbf{A}_{k-1}$ links $\mathbf{x}_k$ to $\mathbf{x}_{k-1}$, the states of an assembly over two stations.

In order to express the state space variation model in the same format as Eq. (1), we reformulate Eq. (5) into an input-output linear model by eliminating all intermediate state variables $\mathbf{x}_k$. Assume that $\mathbf{x}_0=\mathbf{0}$ and sensors are placed at Station N. We have

$$\mathbf{y}_N=\sum_{k=1}^{N}\mathbf{C}_N\mathbf{\Phi}_{N,k}\mathbf{B}_k\mathbf{u}_k+\sum_{k=1}^{N}\mathbf{C}_N\mathbf{\Phi}_{N,k}\mathbf{w}_k+\mathbf{v}_N, \tag{6}$$

where $\mathbf{\Phi}_{N,k}\equiv\mathbf{A}_{N-1}\cdots\mathbf{A}_k$ for $N>k$ and $\mathbf{\Phi}_{k,k}\equiv\mathbf{I}$. Further define $\mathbf{\Gamma}$ and $\mathbf{\Psi}$ as

$$\begin{aligned}\mathbf{\Gamma}&\equiv[\mathbf{C}_N\mathbf{\Phi}_{N,1}\mathbf{B}_1\ \ \mathbf{C}_N\mathbf{\Phi}_{N,2}\mathbf{B}_2\ \cdots\ \mathbf{C}_N\mathbf{B}_N] \quad \text{and}\\ \mathbf{\Psi}&\equiv[\mathbf{C}_N\mathbf{\Phi}_{N,1}\ \ \mathbf{C}_N\mathbf{\Phi}_{N,2}\ \cdots\ \mathbf{C}_N].\end{aligned} \tag{7}$$

This input-output relationship is of the same form as Eq. (1),

$$\mathbf{y}=\mathbf{D}\mathbf{u}+\mathbf{v}, \tag{8}$$

where $\mathbf{u}^T\equiv[\mathbf{u}_1^T\cdots\mathbf{u}_N^T\,\mathbf{w}_1^T\cdots\mathbf{w}_N^T]$, $\mathbf{D}\equiv[\mathbf{\Gamma}\ \mathbf{\Psi}]$, and the subscript N (a station index) is dropped from $\mathbf{y}$ and $\mathbf{v}$ without causing any ambiguity. When the higher order terms and process background noise represented by $\mathbf{w}_k$ are negligible, i.e., $\mathbf{u}^T=[\mathbf{u}_1^T\cdots\mathbf{u}_N^T]$, Eq. (8) further simplifies to

$$\mathbf{y}=\mathbf{\Gamma}\mathbf{u}+\mathbf{v}. \tag{9}$$

In this paper, we focus on the model in Eq. (9). The approaches developed for Eq. (9) can be easily extended to the model in Eq. (8), because they share the same model structure.

In our example of the two-station assembly process, the measurement station (Station II) is in a well-controlled environment, and we only consider variation sources associated with locators in Station I (i.e., fixture errors 1–9). Thus, $\mathbf{u}_2=0$, and Eq. (4) becomes

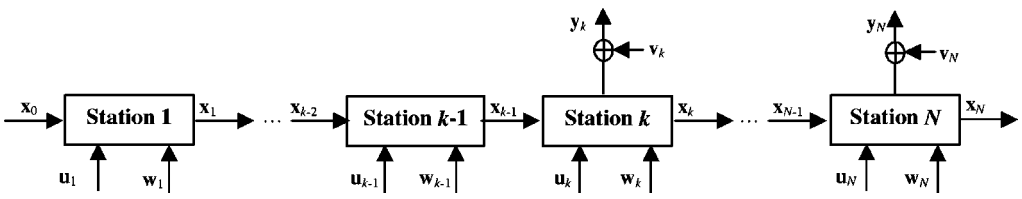

Fig. 3 Diagram of a multi-station discrete-part manufacturing process

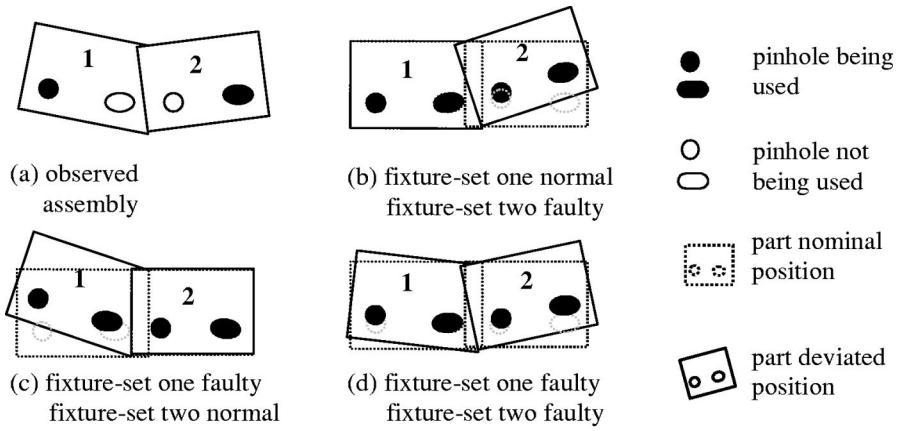

Fig. 4 Multiple possibilities of fixture errors due to re-orientation

$$\mathbf{y}_2=[\mathbf{C}_2\mathbf{A}_1\mathbf{B}_1 \quad \mathbf{C}_2\mathbf{B}_2]\cdot\begin{bmatrix}\mathbf{u}_1\\ \mathbf{u}_2\end{bmatrix}+\mathbf{v}_2=\mathbf{C}_2\mathbf{A}_1\mathbf{B}_1\mathbf{u}_1+\mathbf{v}_2, \tag{10}$$

where the diagnostic matrix $\mathbf{D}=\mathbf{\Gamma}=\mathbf{C}_2\mathbf{A}_1\mathbf{B}_1$. The numerical expression for $\mathbf{\Gamma}$ for this two-station assembly process is provided in Appendix A1. It can be verified that the columns of $\mathbf{\Gamma}$ are linearly dependent ($\mathbf{\Gamma}^T\mathbf{\Gamma}$ is singular) so that the deviation LS estimator is not applicable.

The singularity problem is quite common in multi-station systems, especially when we include a comprehensive set of fixture errors in the model, and may be unavoidable regardless of how many sensors are used. The simple example in Fig. 4 illustrates the reasons why. Suppose the assembly deviation shown in Fig. 4(a) is observed at measurement Station $k+1$. Any of the Station k fixture error scenarios illustrated in Figs. 4(b), 4(c), and 4(d) could have resulted in the assembly deviation in Fig. 4(a). Recall that the assembly deviation observed at measurement Station $k+1$ is related to the fixture errors incurred at the previous station via the model $\mathbf{y}_{k+1}=\mathbf{C}_{k+1}\mathbf{A}_k\mathbf{B}_k\mathbf{u}_k=\mathbf{\Gamma}_k\mathbf{u}_k$ if the measurement station is free of fixture errors. The preceding observation that any of the three fixture error scenarios could have resulted in the same observed assembly deviation means that, given $\mathbf{y}_{k+1}$, there is no unique solution for $\mathbf{u}_k$. Mathematically, this means that the columns of $\mathbf{\Gamma}_k$ are linearly dependent, so that $\mathbf{\Gamma}_k^T\mathbf{\Gamma}_k$ is singular. Because these conclusions clearly hold regardless of how many sensors we add at the measurement Station $k+1$, the only way to avoid a nonsingular system in this case is to add sensors to the assembly Station k. If this is not possible, then the deviation LS estimator cannot be applied.

This singularity problem in multi-station assembly processes was also illustrated in the examples presented by Carlson et al. [8]. With the fixture errors that are included in the error propagation models developed in [17,18,20–22], the diagnostic matrices ($\mathbf{\Gamma}_k$'s) are all less than full rank.

3 Variation Diagnosis

3.1 Variance LS Estimator. Section 2 presented an example for multi-station assembly in which $\mathbf{A}_k$ and $\mathbf{\Gamma}^T\mathbf{\Gamma}$ are both singular. Thus, the deviation LS estimator outlined in (DP1)–(DP3) cannot be applied. This section develops an alternative approach that circumvents this problem. Taking the covariance matrix for both sides of Eq. (9) gives

$$\mathbf{\Sigma}_y=\mathbf{\Gamma}\mathbf{\Sigma}_u\mathbf{\Gamma}^T+\sigma_v^2\mathbf{I}, \tag{11}$$

where $\mathbf{\Sigma}_{(\cdot)}$ is the covariance matrix of a random vector. Since fixture errors associated with different fixture locators are assumed physically independent, $\mathbf{\Sigma}_u=\mathrm{diag}\{\sigma_1^2\,\sigma_2^2\cdots\sigma_p^2\}$ is diagonal, where p is the number of fixture errors included in the model. Define $\boldsymbol{\sigma}^2\equiv[\sigma_1^2\cdots\sigma_p^2\,\sigma_v^2]^T$ as the vector of variance components to be estimated.

Equation (11) can be written as

$$\mathbf{\Sigma}_y=\sum_{i=1}^{p}(\boldsymbol{\gamma}_i\boldsymbol{\gamma}_i^T)\sigma_i^2+\sigma_v^2\mathbf{I} \tag{12}$$

where $\boldsymbol{\gamma}_i$ is the ith column vector of $\mathbf{\Gamma}$. In practice, the population covariance $\mathbf{\Sigma}_y$ is estimated by the sample covariance matrix

$$\mathbf{S}_y=\frac{1}{M-1}\sum_{t=1}^{M}(\mathbf{y}(t)-\overline{\mathbf{y}})(\mathbf{y}(t)-\overline{\mathbf{y}})^T=\mathbf{\Sigma}_y+\mathbf{E}, \tag{13}$$

where $\mathbf{E}$ denotes the estimation error matrix. If we define $\mathbf{V}_i\equiv\boldsymbol{\gamma}_j\boldsymbol{\gamma}_j^T$ for $i=1,\ldots,p$, $\mathbf{V}_{p+1}\equiv\mathbf{I}$, and $\sigma_{p+1}^2\equiv\sigma_v^2$, Eqs. (12) and (13) become

$$\mathbf{S}_y=\sum_{i=1}^{p+1}\mathbf{V}_i\sigma_i^2+\mathbf{E}. \tag{14}$$

In light of this, one approach for estimating the variance components is to choose $\hat{\boldsymbol{\sigma}}^2$ (the "$\wedge$" symbol denotes an estimate) to minimize the sum of the squares of the elements of the error matrix $\mathbf{S}_y-\Sigma_{i=1}^{p+1}\mathbf{V}_i\hat{\sigma}_i^2$. For square matrices $\mathbf{A}$ and $\mathbf{B}$ of compatible dimension, define the matrix inner product $\langle\mathbf{A},\mathbf{B}\rangle=\mathrm{tr}(\mathbf{A}^T\mathbf{B})$ and the associated matrix norm $\|\mathbf{A}\|^2=\langle\mathbf{A},\mathbf{A}\rangle$, which is exactly sum of the squares of the elements of $\mathbf{A}$. Using standard results for least squares estimation in inner-product spaces [23], the estimates in this case must satisfy the so-called normal equations

$$\mathbf{\Pi}\hat{\boldsymbol{\sigma}}^2=\mathbf{b}, \tag{15}$$

where the notation is as follows. $\mathbf{\Pi}$ is the Gram matrix, defined so that the ith-row, jth-column element is $\langle\mathbf{V}_i,\mathbf{V}_j\rangle$ for $1\leqslant i,j\leqslant p+1$. The $(p+1)$-length column vector $\mathbf{b}$ is defined so that its ith element is $\langle\mathbf{V}_i,\mathbf{S}_y\rangle$. For the particular inner product defined above, it can be verified that

$$\mathbf{\Pi}=\begin{bmatrix}(\boldsymbol{\gamma}_1^T\boldsymbol{\gamma}_1)^2 & \cdots & (\boldsymbol{\gamma}_1^T\boldsymbol{\gamma}_p)^2 & \boldsymbol{\gamma}_1^T\boldsymbol{\gamma}_1\\ \vdots & & & \vdots\\ (\boldsymbol{\gamma}_1^T\boldsymbol{\gamma}_p)^2 & \cdots & (\boldsymbol{\gamma}_p^T\boldsymbol{\gamma}_p)^2 & \boldsymbol{\gamma}_p^T\boldsymbol{\gamma}_p\\ \boldsymbol{\gamma}_1^T\boldsymbol{\gamma}_1 & \cdots & \boldsymbol{\gamma}_p^T\boldsymbol{\gamma}_p & n\end{bmatrix} \quad \text{and}$$

$$\mathbf{b}=\begin{bmatrix}\boldsymbol{\gamma}_1^T\mathbf{S}_y\boldsymbol{\gamma}_1\\ \vdots\\ \boldsymbol{\gamma}_p^T\mathbf{S}_y\boldsymbol{\gamma}_p\\ \mathrm{tr}(\mathbf{S}_y)\end{bmatrix}. \tag{16}$$

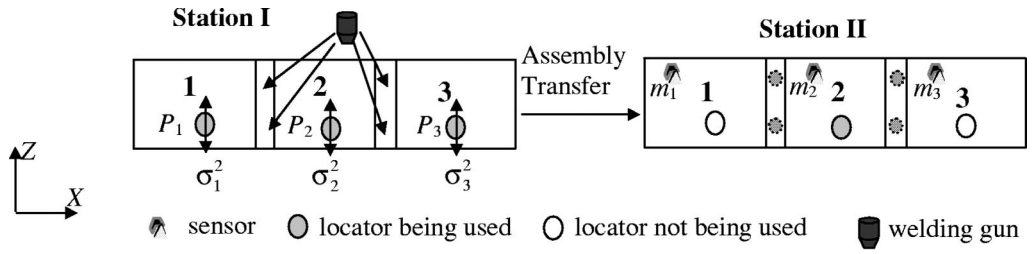

Fig. 5 A three-panel two-station assembly process

When $\mathbf{\Pi}$ is nonsingular, or equivalently when the matrices $\boldsymbol{\gamma}_1\boldsymbol{\gamma}_1^T, \ldots, \boldsymbol{\gamma}_p\boldsymbol{\gamma}_p^T$, and $\mathbf{I}$ are linearly independent, $\hat{\boldsymbol{\sigma}}^2 = \mathbf{\Pi}^{-1}\mathbf{b}$ is a unique solution to Eq. (15). We refer to this approach as the "variance LS estimator."

3.2 Diagnosability of Deviation LS Estimator and Variance LS Estimator. The diagnosability condition required for a variance LS estimator is different from that required for a deviation LS estimator. For the variance LS estimator, the matrix $\mathbf{\Pi}$ must be of full rank in order for Eq. (15) to yield a unique solution. For the deviation LS estimator, the matrix $\mathbf{\Gamma}^T\mathbf{\Gamma}$ must be of full rank and also $n>p$ in order to yield a unique solution. To more clearly illustrate the difference, consider the simplified example shown in Fig. 5, in which each part has only one degree of freedom and can only translate (no rotation) in the *Z*-direction.

Three locators are used to position the three panels at Station I, and their instantaneous position errors are denoted as $\mathbf{u}_1 = [\delta p_1\ \delta p_2\ \delta p_3]^T$. After the joining operation are finished, the three parts become one subassembly and it is transferred to Station II for measurement. The state vectors are $\mathbf{x}_k = [\delta Z_{1,k}\ \delta Z_{2,k}\ \delta Z_{3,k}]^T$ $(k=1,2)$ and the measurement vectors are $\mathbf{y}_1 = \mathbf{0}$ and $\mathbf{y}_2 = [\delta m_1(Z)\ \delta m_2(Z)\ \delta m_3(Z)]^T$. At Station II, the locating hole on part 2 is used to position the whole assembly. The locator on Station II is assumed to be free of positioning errors (i.e., $\mathbf{u}_2 = \mathbf{0}$).

When this three-panel assembly is transferred to Station II, it undergoes a translation by the amount $-\delta Z_{2,1}$, which can be represented as

$$\mathbf{x}_2 = \mathbf{x}_1 + \begin{bmatrix} 0 & -1 & 0 \\ 0 & -1 & 0 \\ 0 & -1 & 0 \end{bmatrix}\mathbf{x}_1 = \begin{bmatrix} 1 & -1 & 0 \\ 0 & 0 & 0 \\ 0 & -1 & 1 \end{bmatrix}\mathbf{x}_1 = \mathbf{A}\mathbf{x}_1. \quad (17)$$

Because $\mathbf{y}_2 = \mathbf{x}_2 + \mathbf{v}$ at Station II, the state space model becomes $\mathbf{x}_1 = \mathbf{u}_1$, $\mathbf{x}_2 = \mathbf{A}_1\mathbf{x}_1$ and $\mathbf{y}_2 = \mathbf{x}_2 + \mathbf{v}$. The linear diagnostic model for this two-station process becomes

$$\mathbf{y}_2 = \mathbf{A}_1\mathbf{u}_1 + \mathbf{v}. \quad (18)$$

Relating this to the model in Eq. (1), we have $\mathbf{D} = \mathbf{\Gamma} = \mathbf{A}_1$, where $\mathbf{A}_1$ shown above is clearly singular. However,

$$\mathbf{\Pi} = \begin{bmatrix} 1 & 1 & 0 & 1 \\ 1 & 4 & 1 & 2 \\ 0 & 1 & 1 & 1 \\ 1 & 2 & 1 & 3 \end{bmatrix} \quad (19)$$

is of full rank. Consequently, the variance vector $\boldsymbol{\sigma}^2$ can be diagnosed using the variance LS estimator in Eq. (15), but not using the deviation LS estimator.

An explanation for diagnosability of variance vector $\boldsymbol{\sigma}^2$ using the variance LS estimator is apparent from the covariance matrix

$$\mathbf{\Sigma}_y = \begin{bmatrix} \sigma_1^2+\sigma_2^2+\sigma_v^2 & 0 & \sigma_2^2 \\ 0 & \sigma_v^2 & 0 \\ \sigma_2^2 & 0 & \sigma_3^2+\sigma_2^2+\sigma_v^2 \end{bmatrix} \quad (20)$$

for this single degree of freedom assembly. The diagonal elements in $\mathbf{\Sigma}_y$ only provide information regarding the summation of the fixture error variance components $\sigma_1^2+\sigma_2^2$ and $\sigma_3^2+\sigma_2^2$, as well as the noise variance σ_v^2. The non-zero off-diagonal element, which is the covariance between $\delta m_1(z)$ and $\delta m_3(z)$, provides extra information. In Station II, $\delta m_1(z) = \delta p_1 - \delta p_2$ and $\delta m_3(z) = \delta p_3 - \delta p_2$, so that $\mathrm{cov}(\delta m_1(z), \delta m_3(z)) = \mathrm{var}(\delta p_2) = \sigma_2^2$ (recall that δp_1 and δp_3 are assumed independent). This extra piece of information is utilized by the variance LS estimator so that variance components are diagnosable. The discussion so far did not include the fixture error $\mathbf{u}_2$ in Station II. A straightforward extension that includes $\mathbf{u}_2$ would result in the same conclusion.

Another way of viewing the difference between these two estimators is the following: a variance LS estimator first calculates covariance matrices of $\mathbf{u}$ and $\mathbf{y}$, and then applies the LS criterion on the sample covariance matrices, whereas a deviation LS estimator first calculates the LS estimates for the individual error vectors $\{\hat{\mathbf{u}}(t)\}_{t=1}^M$, and then calculated the variances of $\mathbf{u}$ from $\{\hat{\mathbf{u}}(t)\}_{t=1}^M$. Because estimating $\{\hat{\mathbf{u}}(t)\}_{t=1}^M$ requires more information than simply estimating its covariance matrix, it is not surprising that the deviation LS estimator requires a stronger diagnosability condition than the variance LS estimator. This is stated in the following theorem, the proof of which is included in Appendix A2.

Theorem 1. If $\mathbf{\Gamma}^T\mathbf{\Gamma}$ is of full rank and $n>p$, then $\mathbf{\Pi}$ is of full rank.

The significance of Theorem 1 is that a unique variance LS estimator exists whenever a unique deviation LS exists. The converse, however, is not necessarily true. As illustrated in the preceding example, there are situations where the variance LS estimator is unique but the deviation LS estimator is not.

3.3 Effect of System Structure Modeled by $\mathbf{\Gamma}$ on Variance Estimation. The performance of the deviation LS estimator will deteriorate for "ill-conditioned" systems, even if $\mathbf{\Gamma}^T\mathbf{\Gamma}$ is not exactly singular. The most common criteria [24] used to quantify how ill-conditioned a system is include $\mathrm{tr}((\mathbf{\Gamma}^T\mathbf{\Gamma})^{-1})$, $\mathrm{cond}(\mathbf{\Gamma}^T\mathbf{\Gamma})$, and $\det((\mathbf{\Gamma}^T\mathbf{\Gamma})^{-1})$, where $\mathrm{cond}(\cdot)$ and $\det(\cdot)$ are the condition number and the determinant of a matrix, respectively. These three measures are related to each other through the eigenvalues of $\mathbf{\Gamma}^T\mathbf{\Gamma}$, which we denote $\{\lambda_i\}_{i=1}^p$. The relationship is

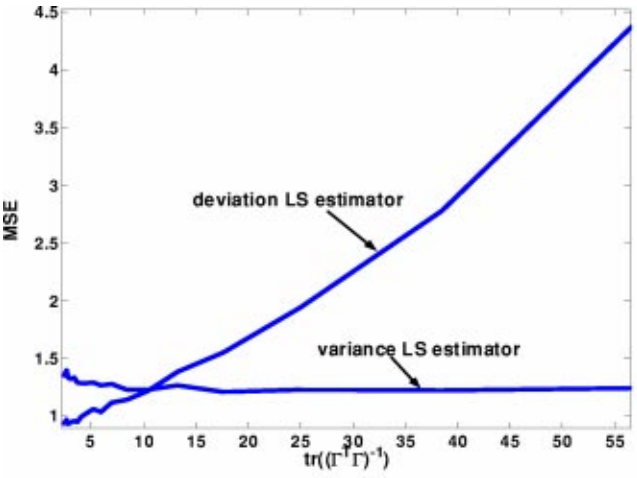

Fig. 6 MSE vs tr$((\mathbf{\Gamma}^T\mathbf{\Gamma})^{-1}$)

$$\mathrm{tr}((\mathbf{\Gamma}^T\mathbf{\Gamma})^{-1}) = \sum_{i=1}^{p} \frac{1}{\lambda_i},$$

$$\det((\mathbf{\Gamma}^T\mathbf{\Gamma})^{-1}) = \prod_{i=1}^{p} \frac{1}{\lambda_i}, \quad \text{and}$$

$$cond(\mathbf{\Gamma}^T\mathbf{\Gamma}) = \frac{\lambda_{\max}}{\lambda_{\min}}. \tag{21}$$

The larger these measures are, the more ill-conditioned the system is. Since $\mathbf{\Gamma}^T\mathbf{\Gamma}$ is non-negative definite, all eigenvalues must be non-negative. The system is singular when these measures are infinite, or equivalently, when one or more eigenvalues are exactly zero. Throughout the remainder of the paper, we use $\mathrm{tr}((\mathbf{\Gamma}^T\mathbf{\Gamma})^{-1})$ as the measure of how ill-conditioned a system is.

The following simulations were used to investigate the extent to which both estimators are affected as the system changes from being well-conditioned to being ill-conditioned. The following parameters were used: $n=6$, $p=3$, $M=50$, $\sigma_v^2=0.25$, $\{\sigma_j^2\}_{j=1}^3 = [1,4,9]$, and

$$\mathbf{\Gamma}^T = \begin{bmatrix} 1 & 1 & 0 & 0 & 0 & 0 \\ -1 & -1 & a & a & -1 & -1 \\ 0 & 0 & 0 & 0 & 1 & 1 \end{bmatrix}, \tag{22}$$

where a was varied from 1 to 0.1 so that the value of $\mathrm{tr}((\mathbf{\Gamma}^T\mathbf{\Gamma})^{-1})$ changes accordingly. For each a, a Monte Carlo simulation with $K=5{,}000$ replicates was conducted for each estimator. The performance measure is the mean square error (MSE) of the estimates

$$\mathrm{MSE} \equiv \frac{1}{p+1} \sum_{j=1}^{p+1} \left\{ \frac{1}{K} \sum_{k=1}^{K} (\hat{\sigma}_{j,k}^2 - \sigma_j^2)^2 \right\}, \tag{23}$$

where $\hat{\sigma}_{j,k}^2$ is the estimate of σ_j^2 for the kth replicate.

Figure 6 shows the MSEs of two estimators vs. the values of $\mathrm{tr}((\mathbf{\Gamma}^T\mathbf{\Gamma})^{-1})$ as a is varied. From this, the following observations can be made: (a) The performance of the deviation LS estimator deteriorates rapidly (the MSE increases) as $\mathrm{tr}((\mathbf{\Gamma}^T\mathbf{\Gamma})^{-1})$ increases. In contrast, the MSE of the variance LS estimator is largely independent of $\mathrm{tr}((\mathbf{\Gamma}^T\mathbf{\Gamma})^{-1})$. Clearly, the variance LS estimator is less sensitive to linear dependencies in system structure. (b) Although the variance LS estimator performs better for ill-conditioned systems, the deviation LS estimator has a smaller MSE value when $\mathrm{tr}((\mathbf{\Gamma}^T\mathbf{\Gamma})^{-1})$ is small (e.g., less than 10). We may conclude that the deviation LS estimator can outperform a variance LS estimator for a well-conditioned system. For an ill-conditioned system, however, the variance LS estimator will perform substantially better. In the following subsection, we present a modified version of the variance LS estimator that performs uniformly better than the deviation LS estimator.

Although the performances of these two estimators will generally differ, the estimators are actually equivalent in the special case that all columns of $\mathbf{\Gamma}$ are orthogonal, i.e., when $\boldsymbol{\gamma}_i^T\boldsymbol{\gamma}_j=0$, $\forall i \neq j$. This obviously requires that $\mathbf{\Gamma}^T\mathbf{\Gamma}$ is of full rank. This is stated as Theorem 2, the proof of which is included in Appendix A3.

Theorem 2. If $n>p$, and $\boldsymbol{\gamma}_i^T\boldsymbol{\gamma}_j=0$, $\forall i \neq j$, the variance LS estimator in Eq. (15) is the same as the deviation LS estimator described in (DP1)–(DP3).

3.4 Modified Procedures to Enhance the Performance of the Variance LS Estimator. One observation in the previous section was that the variance LS estimator may perform worse than the deviation LS estimator for a well-conditioned system. This motivates the following algorithm for improving the performance of the variance LS estimator. A more general version of the algorithm was originally proposed by Anderson [25] as an approximate maximum likelihood method. For the present case, the expressions required in Step 2 of the algorithm simplify considerably to those shown below. The algorithm iterates over the following two steps until convergence.

Modified Procedure 1 (MP1)

1) Based on the estimate $\hat{\boldsymbol{\sigma}}^2$ at the previous iteration, calculate the following estimate of the covariance matrix [see Eq. (12)]

$$\hat{\mathbf{\Sigma}}_y = \sum_{i=1}^{p} (\boldsymbol{\gamma}_i\boldsymbol{\gamma}_i^T)\hat{\sigma}_i^2 + \hat{\sigma}_v^2\mathbf{I}$$

2) Solve the equation $\mathbf{\Pi}^*\hat{\boldsymbol{\sigma}}^2 = \mathbf{b}^*$ for the new estimate $\hat{\boldsymbol{\sigma}}^2$ at the current iteration, where

$$\mathbf{\Pi}^* = \begin{bmatrix} (\boldsymbol{\gamma}_1^T\hat{\mathbf{\Sigma}}_y^{-1}\boldsymbol{\gamma}_1)^2 & \cdots & (\boldsymbol{\gamma}_1^T\hat{\mathbf{\Sigma}}_y^{-1}\boldsymbol{\gamma}_p)^2 & \boldsymbol{\gamma}_1^T\hat{\mathbf{\Sigma}}_y^{-2}\boldsymbol{\gamma}_1 \\ \vdots & & & \vdots \\ (\boldsymbol{\gamma}_1^T\hat{\mathbf{\Sigma}}_y^{-1}\boldsymbol{\gamma}_p)^2 & \cdots & (\boldsymbol{\gamma}_p^T\hat{\mathbf{\Sigma}}_y^{-1}\boldsymbol{\gamma}_p)^2 & \boldsymbol{\gamma}_p^T\hat{\mathbf{\Sigma}}_y^{-2}\boldsymbol{\gamma}_p \\ \boldsymbol{\gamma}_1^T\hat{\mathbf{\Sigma}}_y^{-2}\boldsymbol{\gamma}_1 & \cdots & \boldsymbol{\gamma}_p^T\hat{\mathbf{\Sigma}}_y^{-2}\boldsymbol{\gamma}_p & \mathrm{tr}(\hat{\mathbf{\Sigma}}_y^{-2}) \end{bmatrix} \quad \text{and}$$

$$\mathbf{b}^* = \begin{bmatrix} \boldsymbol{\gamma}_1^T\hat{\mathbf{\Sigma}}_y^{-1}\mathbf{S}_y\hat{\mathbf{\Sigma}}_y^{-1}\boldsymbol{\gamma}_1 \\ \vdots \\ \boldsymbol{\gamma}_p^T\hat{\mathbf{\Sigma}}_y^{-1}\mathbf{S}_y\hat{\mathbf{\Sigma}}_y^{-1}\boldsymbol{\gamma}_p \\ \mathrm{tr}(\hat{\mathbf{\Sigma}}_y^{-2}\mathbf{S}_y) \end{bmatrix}.$$

At the initial iteration, we can use the estimate $\hat{\boldsymbol{\sigma}}^2$ from the variance LS algorithm of Eq. (15). Convergence usually occurs after only one or two iterations. In all of the subsequent simulations, only a single iteration was used.

The MP1 algorithm bears a strong resemblance to the variance LS algorithm of Eq. (15). Suppose we transform Eq. (14) by pre- and post-multiplying both sides by $\hat{\mathbf{\Sigma}}_y^{-1/2}$, which gives

$$\hat{\mathbf{\Sigma}}_y^{-1/2}\mathbf{S}_y\hat{\mathbf{\Sigma}}_y^{-1/2} = \sum_{i=1}^{p+1} \hat{\mathbf{\Sigma}}_y^{-1/2}\mathbf{V}_i\hat{\mathbf{\Sigma}}_y^{-1/2}\sigma_i^2 + \hat{\mathbf{\Sigma}}_y^{-1/2}\mathbf{E}\hat{\mathbf{\Sigma}}_y^{-1/2}.$$

It is straightforward to verify that $\mathbf{\Pi}^*$ is the Gram matrix of inner products for the transformed matrices $\{\hat{\mathbf{\Sigma}}_y^{-1/2}\mathbf{V}_i\hat{\mathbf{\Sigma}}_y^{-1/2} : i = 1,2,\ldots,p+1\}$ and that the elements of $\mathbf{b}^*$ are the inner products $\langle \hat{\mathbf{\Sigma}}_y^{-1/2}\mathbf{S}_y\hat{\mathbf{\Sigma}}_y^{-1/2}, \hat{\mathbf{\Sigma}}_y^{-1/2}\mathbf{V}_i\hat{\mathbf{\Sigma}}_y^{-1/2} \rangle$ for the transformed matrices.

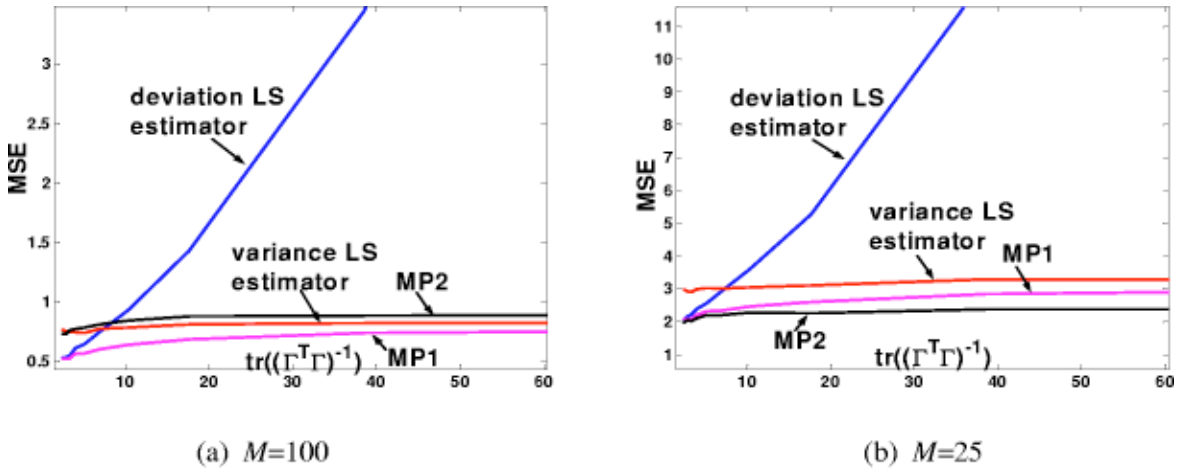

Fig. 7 The performance comparison of variance estimators

At each iteration, the MP1 algorithm is therefore the least squares solution that minimizes the norm of the transformed error matrix $\hat{\boldsymbol{\Sigma}}_y^{-1/2}\mathbf{S}_y\hat{\boldsymbol{\Sigma}}_y^{-1/2}-\Sigma_{i=1}^{p+1}\hat{\boldsymbol{\Sigma}}_y^{-1/2}\mathbf{V}_i\hat{\boldsymbol{\Sigma}}_y^{-1/2}\hat{\sigma}_i^2$. The transformation by $\hat{\boldsymbol{\Sigma}}_y^{-1/2}$ can be viewed as weighted least squares [26], since the elements of $\hat{\boldsymbol{\Sigma}}_y^{-1/2}\mathbf{E}\hat{\boldsymbol{\Sigma}}_y^{-1/2}$ are uncorrelated with equal variance. Note that the elements of the untransformed error matrix $\mathbf{E}$ are neither uncorrelated nor have equal variance.

The MP1 algorithm can substantially improve the performance over the variance LS estimator, especially for a well-conditioned system. In fact, Anderson [25] has shown that the MP1 estimator is asymptotically efficient. The improvement is illustrated via simulation using the same $\boldsymbol{\Gamma}$ as in Section 3.3 (except that we now use a larger sample size of $M=100$). The simulation results are shown in Fig. 7(a), which shows that the MP1 estimator has uniformly smaller MSE values than the other estimators.

If $\hat{\boldsymbol{\Sigma}}_y$ is positive definite at each step of the iteration, $\boldsymbol{\Pi}^*$ will be full rank if and only if $\boldsymbol{\Pi}$ is full rank. Thus, the conditions required for the MP1 algorithm to produce a unique estimate are identical to the conditions required by the variance LS algorithm, provided that $\hat{\boldsymbol{\Sigma}}_y$ remains positive definite at each iteration. This is not guaranteed, however, because elements of $\hat{\boldsymbol{\sigma}}^2$ may take on negative values. This is more likely to occur when the sample size is relatively small and the true variance components are close to zero. The negativity of estimates is a problem in almost all of the variance estimation algorithms (the deviation LS estimator cannot avoid negative estimates, either). The most popular approach to enforce non-negativity is to replace the negative elements in $\hat{\boldsymbol{\sigma}}^2$ with zeros. As long as $\sigma_v^2>0$, $\hat{\boldsymbol{\Sigma}}_y$ is then guaranteed to be positive definite. If σ_v^2 becomes negative and is replaced by 0, the pseudo-inverse of $\hat{\boldsymbol{\Sigma}}_y$ can be used in step 2.

Rao and Kleffe developed a different variance estimation approach [[27], Eq. 9.1.8] that avoids negative estimates. Their iterative algorithm will give positive variance component estimates, provided that the initial estimates are positive. This procedure is less intuitive and its development is rather mathematically involved. Consequently, we simply present the final form of the algorithm for practical use. Note that the form of the algorithm in Rao and Kleffe's Eq. 9.1.8 is much more complex than the algorithm below. The reason is that for the particular model in Eq. (1), the expressions simplify considerably to those shown below.

Modified Procedure 2 (MP2)

(M1) Select an initial $\hat{\boldsymbol{\sigma}}_0^2=[\hat{\sigma}_{1,0}^2\cdots\hat{\sigma}_{p,0}^2\,\hat{\sigma}_{v,0}^2]^T$ with all positive values.

(M2) Calculate $\hat{\boldsymbol{\Sigma}}_{y,0}=\boldsymbol{\Gamma}\cdot\hat{\boldsymbol{\Sigma}}_{u,0}\cdot\boldsymbol{\Gamma}^T+\hat{\sigma}_{v,0}^2\cdot\mathbf{I}$, where $\hat{\boldsymbol{\Sigma}}_{u,0}=\mathrm{diag}\{\hat{\sigma}_{1,0}^2\cdots\hat{\sigma}_{p,0}^2\}$.

(M3) Solve the following set of linear equations for $j=0$ and 1.

$$\hat{\sigma}_{i,j+1}^2=\hat{\sigma}_{i,j}^2\cdot(\mathrm{tr}(\hat{\boldsymbol{\Sigma}}_{y,j}^{-1}\cdot\boldsymbol{\gamma}_i\boldsymbol{\gamma}_i^T))^{-1}\cdot\mathrm{tr}(\hat{\boldsymbol{\Sigma}}_{y,j}^{-1}\cdot\boldsymbol{\gamma}_i\boldsymbol{\gamma}_i^T\cdot\hat{\boldsymbol{\Sigma}}_{y,j}^{-1}\cdot\mathbf{S}_y),\quad i=1,\ldots,p,\quad\text{and}$$

$$\hat{\sigma}_{v,j+1}^2=\hat{\sigma}_{v,j}^2\cdot(\mathrm{tr}(\hat{\boldsymbol{\Sigma}}_{y,j}^{-1}))^{-1}\cdot\mathrm{tr}(\hat{\boldsymbol{\Sigma}}_{y,j}^{-1}\cdot\hat{\boldsymbol{\Sigma}}_{y,j}^{-1}\cdot\mathbf{S}_y).\qquad(24)$$

The $\{\hat{\sigma}_{i,j}^2\}_{i=1}^p$ and $\hat{\sigma}_{v,j}^2$ in MP2 will remain positive as long as the initial values of $\hat{\boldsymbol{\sigma}}_0^2$ are chosen positive. The usual choice is to let $\hat{\sigma}_{i,0}^2=\hat{\sigma}_{v,0}^2=1$, for $i=1,\ldots,p$. The solution $[\hat{\sigma}_{1,2}^2\cdots\hat{\sigma}_{p,2}^2\,\hat{\sigma}_{v,2}^2]^T$ is the final estimate. The results for the MP2 estimator in the situation described in the preceding simulation were also included in Fig. 7. For the relatively small sample size of $M=25$, the MP2 estimator outperforms the other estimators. For the more typical sample size of $M=100$, however, the MP1 estimator performs better than the MP2 estimator. The reason is that the MP2 estimator forces a bias in order to make $\hat{\boldsymbol{\sigma}}^2$ positive, and this bias does not disappear as sample size increases. In contrast, the MP1 estimator is unbiased and consistent, meaning that its variance approaches zero as sample size increases. Consequently, the MP2 estimator is only recommended if sample size is very small.

4 Examples

In this section, the estimators are applied to fixture error diagnosis in various automotive body assembly problems. Monte Carlo simulations with 5,000 replicates were conducted in a MATLAB environment, and fixture errors were assumed to follow a normal distribution in all cases. For detailed descriptions of the processes, the reader is referred to the various references cited below. For convenience, the diagnostic matrix $\boldsymbol{\Gamma}$ is provided below for each situation.

4.1 Assembly System With an Orthogonal Diagnostic Matrix.

The automotive assembly process was described in considerable detail in Apley and Shi [5]. In Section 5 of their paper, they apply the deviation LS estimator to diagnosing errors in fixtures that locate the side frames of a car body. They assumed the linear structured model of Eq. (9) to represent the effects of fixture errors on dimensional measurements. There were 14 measurements ($n=14$) and two potential fixture errors ($p=2$). The matrix $\boldsymbol{\Gamma}$ (which is the $\mathbf{C}$ matrix in their paper) was through kinematics analysis determined to be

$$\mathbf{\Gamma}^T=\begin{bmatrix} .354 & .354 & .354 & .354 & .354 & .354 & .354 & .354 & 0 & 0 & 0 & 0 & 0 & 0 \\ .057 & -.026 & 0 & -.004 & .046 & -.087 & -.024 & .043 & .187 & .361 & 0 & .535 & .495 & .536 \end{bmatrix}. \tag{25}$$

This $\mathbf{\Gamma}$ matrix is of full column rank and $n>p$, suggesting that the variance LS estimator and the deviation LS estimator can both be applied. We also have $\mathrm{tr}((\mathbf{\Gamma}^T\mathbf{\Gamma})^{-1})=1.99$, indicating that the system is well-conditioned.

For this side-frame assembly system, both deviation LS estimator and variance LS estimator are used to estimate the variance components associated with fixture errors. Five different sample sizes were used ($M=5,10,25,50,100$) in the simulation. From the MSE values shown in Fig. 8, it can be seen that the two estimators have almost identical performance in this example. The reason is that the two columns of $\mathbf{\Gamma}$ are almost orthogonal ($\boldsymbol{\gamma}_1^T\boldsymbol{\gamma}_2=0.018$, $\boldsymbol{\gamma}_1^T\boldsymbol{\gamma}_1=1.0025$, and $\boldsymbol{\gamma}_2^T\boldsymbol{\gamma}_2=0.9999$). This agrees with Theorem 2, which states that the two estimators are equivalent with the columns of $\mathbf{\Gamma}$ are orthogonal.

4.2 Assembly System With a Non-Orthogonal Diagnostic Matrix. Many engineering systems do not result in an orthogonal $\mathbf{\Gamma}$ matrix, in which case the performance of the deviation LS and variance LS estimators will differ. For example, the $\mathbf{\Gamma}$ matrix used in Section 4 of Apley and Shi [5] is

$$\mathbf{\Gamma}^T=\begin{bmatrix} .093 & 0 & -.093 & .093 & 0 & .647 & -.370 & 0 & .647 \\ .577 & 0 & 0 & .577 & 0 & 0 & .577 & 0 & 0 \\ -.120 & 0 & .843 & -.120 & 0 & -.120 & .482 & 0 & -.120 \end{bmatrix}, \tag{26}$$

the columns of which are not orthogonal. In this case, $n=9$, $p=3$, and $\mathrm{tr}((\mathbf{\Gamma}^T\mathbf{\Gamma})^{-1})=3.5$, implying the system is relatively well-conditioned.

Monte Carlo simulations were again conducted, but this time with a sample size of $M=15$. A comparison of the deviation LS estimator, the variance LS estimator, and the MP2 estimator (due to the small sample size) is shown in Table 1. The quantity $(\Sigma_{i=1}^{p+1}\mathrm{var}(\hat{\sigma}_i^2))/(p+1)$ in the third row represents the average sample variance of the estimators for comparison with the MSE. We found that the estimator from MP2 demonstrates slightly more bias than the other two, but has smaller dispersion. Based on the MSE criterion, the MP2 estimator performed the best, followed by the deviation LS estimator.

4.3 Assembly System With a Singular Diagnostic Matrix We next apply the variance estimators to the two-station example introduced in Section 2.2. The $\mathbf{\Gamma}$ matrix for this model is given in Appendix A1. Because the system is singular with $\mathrm{tr}((\mathbf{\Gamma}^T\mathbf{\Gamma})^{-1})=\infty$, the deviation LS estimator cannot be used here. It can be verified that $\mathbf{\Pi}$ is full rank, so that the variance LS estimator and its modified versions are applicable.

As discussed in Section 2, we only consider fixture errors associated with Station I. Hence $p=9$ and $n=18$. Simulations were carried out using a sample size of $M=100$. The variance LS estimator of Eq. (15) and the MP1 and MP2 estimators were compared in this example, and the results are shown in Table 2. In this example, the variance LS estimator and MP1 estimator perform comparably, although the latter has slightly smaller MSE and dispersion. This is consistent with the results shown in Fig. 7(a) as $\mathrm{tr}((\mathbf{\Gamma}^T\mathbf{\Gamma})^{-1})$ increases. The MP2 procedure has the smallest MSE and dispersion among the three. But it also has quite noticeable bias.

Although the MP2 estimator outperformed the MP1 estimator in this example, our experience indicates this is more an exception than the norm. For example, in Fig. 7(a), the MP1 has a smaller MSE value. As another example, suppose we modify the two-station assembly example considered in the preceding paragraph so that we are now only interested in diagnosing the *Z*-direction fixture errors. The $\mathbf{\Gamma}$ matrix in this case is the same as the $\mathbf{\Gamma}$ matrix given in Appendix A1, except that we remove column 1, 4, and 7. It can be verified that that the new $\mathbf{\Gamma}$ matrix is also less than full rank. Repeating the above simulations but with the new $\mathbf{\Gamma}$ matrix, the MSEs for the MP1 and MP2 estimators are 1.197 and 1.215. Thus, the MP1 estimator is slightly more effective than the MP2 estimator in this case.

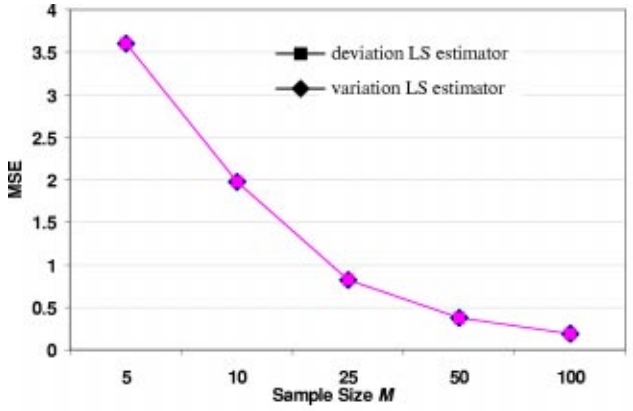

Fig. 8 MSE for the linear system with Γ as in Eq. (25)

Table 1 Comparison of three estimators for the linear system with Γ as in Eq. (26)

	Deviation LS estimator	Variance LS estimator	MP2
$\overline{\hat{\boldsymbol{\sigma}}^2}$	[1.0347 4.0276 3.9965 0.9861]	[1.0015 4.0419 3.9925 0.9854]	[1.0050 3.4421 3.3303 1.0358]
$\frac{\Sigma_{i=1}^{p+1}\mathrm{var}(\hat{\sigma}_i^2)}{p+1}$	1.96	2.10	1.36
MSE	1.96	2.10	1.55

The "true" value of $\boldsymbol{\sigma}^2$ used in the simulation is [1,4,4,1].

Table 2 Comparison of three estimators for the linear system with Γ a singular

	Variance LS estimator	MP1	MP2
$\hat{\boldsymbol{\sigma}}^2$	[0.99814 4.6732 1.6707 3.2344 7.0257 8.988 0.99209 3.9858 5.2822 1.002]	[0.98779 3.9031 1.7135 3.2671 7.0207 9.03 0.99719 4.0153 5.149 1.0001]	[1.1576 3.7646 1.9437 2.6107 6.1577 8.0317 1.0109 3.444 5.3732 1.036]
$\frac{\Sigma_{i=1}^{p+1}\mathrm{var}(\hat{\sigma}_i^2)}{p+1}$	2.731	2.540	0.590
MSE	2.777	2.543	0.844

The "true" values of $\boldsymbol{\sigma}^2$ used in the simulation is [1.00 4.00 1.69 3.24 7.02 9.00 1.00 4.00 5.29 1.00]

5 Concluding Remarks

Singularity is a common problem in engineering systems, in which case the traditional least-squares estimation method cannot be applied effectively. This paper presents a new diagnosability condition and a variance LS estimator that takes into account the covariance between error terms and results in diagnosability for systems that are not diagnosable using traditional LS methods. Two modified versions of the algorithm were also presented to improve the performance of the variance LS estimator.

We note that the presented methods typically require a random sample of 25–50 units. For a dynamic process with tool wear, the process data are inherently autocorrelated. However, since 25–50 units typically translates to production periods of one hour or less, the sampling period will generally be too small to observe any noticeable tool wear effects. Consequently, the methods should still be applicable to diagnosing other types of fixture errors in processes that also experience relatively slow tool wear dynamics (although other methods would be required to diagnose the tool wear itself). For processes with faster tool wear dynamics, recursive estimation methods would need to be developed.

We also point out that the methods are for variance component estimation, as opposed to mean component estimation. Our experience has been that the autobody industry views fixture error variance as more problematic than mean shifts. A sustained, consistent deviation from nominal (i.e., a mean shift) can often be compensated quite easily by process engineers via shimming and other adjustments. In contrast, variation is much more difficult to compensate and requires either some form of on-line feedback control or the removal of the variation root cause. The methods presented in this paper are intended to be a tool to aid in detecting, identifying, and, ultimately, eliminating root causes of random variation.

The examples in this study have been exclusively for fixture error diagnosis in multi-station assembly processes. However, all of the results and conclusions should also hold for other types of error sources and multi-station manufacturing processes, provided that the linear structured model adequately represents the effects of the error sources on the process and product measurements.

Acknowledgment

This research was partially supported by the NSF grants DMI-0217481 and DMI-0093580. The authors also gratefully acknowledge the valuable comments and suggestions from the associate editor and referees.

Appendices

A1 Expression of Matrices for Example in Section 2.

$$\mathbf{A}_1 = \begin{bmatrix} 0 & 0 & 0 & 0 & 0 & 0 & 0 & 0 & 0 & 0 & 0 & 0 \\ 0 & 0 & 0 & 0 & 0 & 0 & 0 & 0 & 0 & 0 & 0 & 0 \\ 0 & 0.0005 & 1 & 1 & 0 & 0 & 0 & 0 & 0 & 0 & -0.0005 & -0.2392 \\ -1 & 0 & 0 & 0 & 1 & 0 & 0 & 0 & 0 & 0 & 0 & 0 \\ 0 & -0.5550 & 0 & 0 & 0 & 1 & 0 & 0 & 0 & 0 & -0.4450 & -222.49 \\ 0 & 0.0005 & 0 & 0 & 0 & 0 & 1 & 0 & 0 & 0 & -0.0005 & -0.2392 \\ -1 & -0.2153 & 0 & 0 & 0 & 0 & 0 & 1 & 0 & 0 & 0.2153 & 107.655 \\ 0 & -0.2392 & 0 & 0 & 0 & 0 & 0 & 0 & 1 & 0 & -0.7608 & -380.38 \\ 0 & 0.0005 & 0 & 0 & 0 & 0 & 0 & 0 & 0 & 0 & -0.0005 & -0.2392 \\ -1 & 0 & 0 & 0 & 0 & 0 & 0 & 0 & 0 & 1 & -0.0005 & 0 \\ 0 & -0.2392 & 0 & 0 & 0 & 0 & 0 & 0 & 0 & 0 & 0.2392 & -380.38 \\ 0 & 0.0005 & 0 & 0 & 0 & 0 & 0 & 0 & 0 & 0 & -0.0005 & 0.7608 \end{bmatrix}_{12\times 12}$$

$$\boldsymbol{\Gamma}=\begin{bmatrix}
0 & 0.1215 & -0.3846 & 0 & 0 & 0 & 0 & 0 & 0.2632\\
0 & 0.0221 & -0.0699 & 0 & 0 & 0 & 0 & 0 & 0.0478\\
0 & 0.1215 & -0.3846 & 0 & 0 & 0 & 0 & 0 & 0.2632\\
0 & -0.1877 & 0.5944 & 0 & 0 & 0 & 0 & 0 & -0.4067\\
0 & -0.0773 & 0.2448 & 0 & 0 & 0 & 0 & 0 & -0.1675\\
0 & -0.3379 & 1.0699 & 0 & 0 & 0 & 0 & 0 & -0.7321\\
0 & 0.1656 & -0.5245 & 0 & 0 & 0 & 0 & 0 & 0.3589\\
0 & -0.3379 & 1.0699 & 0 & 0 & 0 & 0 & 0 & -0.7321\\
0 & 0 & 0 & 0 & 0 & 0 & 0 & 0 & 0\\
0 & -0.2054 & 0.6503 & 0 & 0 & 0 & 0 & 0 & -0.445\\
-1 & -0.311 & 0 & 1 & 0.4 & -0.4 & 0 & 0 & 0.311\\
0 & 0.0574 & 0 & 0 & -0.24 & 1.24 & 0 & 0 & -1.0574\\
-1 & -0.2153 & 0 & 1 & 0 & 0 & 0 & 0 & 0.2153\\
0 & -0.2392 & 0 & 0 & 1 & 0 & 0 & 0 & -0.7608\\
-1 & -0.0957 & 0 & 0 & 0 & 0 & 1 & 0.4 & -0.3043\\
0 & 0.0574 & 0 & 0 & 0 & 0 & 0 & -0.24 & 0.1826\\
-1 & 0 & 0 & 0 & 0 & 0 & 1 & 0 & 0\\
0 & -0.2392 & 0 & 0 & 0 & 0 & 0 & 1 & -0.7608
\end{bmatrix}_{18\times 9}.$$

A2 Proof of Theorem 1. Suppose $\boldsymbol{\Gamma}^T\boldsymbol{\Gamma}$ is of full rank and $n>p$, but that $\boldsymbol{\Pi}$ is singular. Because $\boldsymbol{\Pi}$ is the Gram matrix of $\{\boldsymbol{\gamma}_1\boldsymbol{\gamma}_1^T,\boldsymbol{\gamma}_2\boldsymbol{\gamma}_2^T,\ldots,\boldsymbol{\gamma}_p\boldsymbol{\gamma}_p^T,\mathbf{I}\}$, its singularity implies that $\{\boldsymbol{\gamma}_1\boldsymbol{\gamma}_1^T,\boldsymbol{\gamma}_2\boldsymbol{\gamma}_2^T,\ldots,\boldsymbol{\gamma}_p\boldsymbol{\gamma}_p^T,\mathbf{I}\}$ are linearly dependent. Thus, there exists a set of scalars $\{\alpha_1,\alpha_2,\ldots,\alpha_p,\alpha_{p+1}\}$, not all zero, such that $\boldsymbol{\gamma}_1\boldsymbol{\gamma}_1^T\alpha_1+\boldsymbol{\gamma}_2\boldsymbol{\gamma}_2^T\alpha_2+\ldots+\boldsymbol{\gamma}_p\boldsymbol{\gamma}_p^T\alpha_p=-\mathbf{I}\alpha_{p+1}$. In order for this to hold, we must have $\alpha_{p+1}=0$. Otherwise, $rank(\delta\mathbf{I})=n$, whereas the summation of matrices on the left hand side can have at most rank $p<n$. It follows that $\boldsymbol{\gamma}_1\boldsymbol{\gamma}_1^T\alpha_1+\boldsymbol{\gamma}_2\boldsymbol{\gamma}_2^T\alpha_2+\ldots+\boldsymbol{\gamma}_p\boldsymbol{\gamma}_p^T\alpha_p=\mathbf{0}$, and at least one of the α's (say α_i) is nonzero. Post-multiplying the preceding equation by $\boldsymbol{\gamma}_i$ gives $\boldsymbol{\gamma}_1(\boldsymbol{\gamma}_1^T\boldsymbol{\gamma}_i\alpha_1)+\boldsymbol{\gamma}_2(\boldsymbol{\gamma}_2^T\boldsymbol{\gamma}_i\alpha_2)+\ldots+\boldsymbol{\gamma}_p(\boldsymbol{\gamma}_p^T\boldsymbol{\gamma}_i\alpha_p)=\mathbf{0}$. Because at least one of the coefficients $(\boldsymbol{\gamma}_i^T\boldsymbol{\gamma}_i\alpha_i)$ is nonzero, this implies that the vectors $\{\boldsymbol{\gamma}_1,\boldsymbol{\gamma}_2,\ldots,\boldsymbol{\gamma}_p\}$ are linearly dependent. Their Gram matrix $\boldsymbol{\Gamma}^T\boldsymbol{\Gamma}$ must therefore be singular, which contradicts the condition that $\boldsymbol{\Gamma}^T\boldsymbol{\Gamma}$ is full rank. ◇

A3 Proof of Theorem 2. Utilizing the fact that the columns in $\boldsymbol{\Gamma}$ are orthogonal to each other, i.e., $\boldsymbol{\gamma}_i^T\boldsymbol{\gamma}_j=0,\ \forall i\neq j$, we can re-write Eq. (15) as

$$\begin{bmatrix}
(\boldsymbol{\gamma}_1^T\boldsymbol{\gamma}_1)^2 & \cdots & 0 & \boldsymbol{\gamma}_1^T\boldsymbol{\gamma}_1\\
\vdots & \vdots & \vdots & \vdots\\
0 & \cdots & (\boldsymbol{\gamma}_p^T\boldsymbol{\gamma}_p)^2 & \boldsymbol{\gamma}_p^T\boldsymbol{\gamma}_p\\
\boldsymbol{\gamma}_1^T\boldsymbol{\gamma}_1 & \cdots & \boldsymbol{\gamma}_p^T\boldsymbol{\gamma}_p & n
\end{bmatrix}\cdot\begin{bmatrix}\hat{\sigma}_1^2\\ \vdots\\ \hat{\sigma}_p^2\\ \hat{\sigma}_v^2\end{bmatrix}=\begin{bmatrix}\mathrm{tr}(\boldsymbol{\gamma}_1\boldsymbol{\gamma}_1^T\mathbf{S}_y)\\ \vdots\\ \mathrm{tr}(\boldsymbol{\gamma}_p\boldsymbol{\gamma}_p^T\mathbf{S}_y)\\ \mathrm{tr}(\mathbf{S}_y)\end{bmatrix}. \tag{a1}$$

The above equation is equivalent to

$$\begin{cases}(\boldsymbol{\gamma}_i^T\boldsymbol{\gamma}_i)^2\cdot\hat{\sigma}_i^2+\boldsymbol{\gamma}_i^T\boldsymbol{\gamma}_i\cdot\hat{\sigma}_v^2=\mathrm{tr}(\boldsymbol{\gamma}_i\boldsymbol{\gamma}_i^T\mathbf{S}_y), & i=1,2,\ldots,p\\ \sum_{i=1}^{p}\boldsymbol{\gamma}_i^T\boldsymbol{\gamma}_i\cdot\hat{\sigma}_i^2+n\cdot\hat{\sigma}_v^2=\mathrm{tr}(\mathbf{S}_y).\end{cases} \tag{a2}$$

We can solve $\{\hat{\sigma}_i^2\}_{i=1}^p$ in terms of $\hat{\sigma}_v^2$ from the first equation and substitute it into the second equation. Then, we have

$$\begin{aligned}(n-p)\hat{\sigma}_v^2&=\mathrm{tr}(\mathbf{S}_y)-\sum_{i=1}^{p}\frac{1}{\boldsymbol{\gamma}_i^T\boldsymbol{\gamma}_i}\mathrm{tr}(\boldsymbol{\gamma}_i\boldsymbol{\gamma}_i^T\mathbf{S}_y)\\&=\mathrm{tr}(\mathbf{S}_y)-\mathrm{tr}\left\{\left(\sum_{i=1}^{p}\frac{1}{\boldsymbol{\gamma}_i^T\boldsymbol{\gamma}_i}\boldsymbol{\gamma}_i\boldsymbol{\gamma}_i^T\right)\cdot\mathbf{S}_y\right\}.\end{aligned} \tag{a3}$$

Notice that $\boldsymbol{\Gamma}^T\boldsymbol{\Gamma}$ is a diagonal matrix with $\boldsymbol{\gamma}_i^T\boldsymbol{\gamma}_i$ as its (i,i)th element and $\Sigma_{i=1}^p\omega_i\boldsymbol{\gamma}_i\boldsymbol{\gamma}_i^T=\boldsymbol{\Gamma}\boldsymbol{\Omega}\boldsymbol{\Gamma}^T$, where $\boldsymbol{\Omega}=\mathrm{diag}\{\omega_1\cdots\omega_p\}$ and ω_i, $i=1,\ldots,p$, is an arbitrary real number. Then, we have

$$\sum_{i=1}^{p}\frac{1}{\boldsymbol{\gamma}_i^T\boldsymbol{\gamma}_i}\boldsymbol{\gamma}_i\boldsymbol{\gamma}_i^T=\boldsymbol{\Gamma}(\boldsymbol{\Gamma}^T\boldsymbol{\Gamma})^{-1}\boldsymbol{\Gamma}^T=\boldsymbol{\Gamma}\boldsymbol{\Gamma}^+. \tag{a4}$$

Given all these results, we can write Eq. (a3) as

$$\hat{\sigma}_v^2=\frac{1}{(n-p)}\mathrm{tr}((\mathbf{I}-\boldsymbol{\Gamma}\boldsymbol{\Gamma}^+)\mathbf{S}_y). \tag{a5}$$

It can be further shown that this $\hat{\sigma}_v^2$ is the same as the one in the deviation LS estimator. Substitute $\hat{\mathbf{v}}(t)=\mathbf{y}(t)-\overline{\mathbf{y}}-\boldsymbol{\Gamma}\hat{\mathbf{u}}(t)$ and $\hat{\mathbf{u}}(t)=\boldsymbol{\Gamma}^+(\mathbf{y}(t)-\overline{\mathbf{y}})$ into $\hat{\sigma}_v^2=(\Sigma_{t=1}^M\hat{\mathbf{v}}(t)^T\hat{\mathbf{v}}(t))/((M-1)(n-p))$. It turns out that

$$\begin{aligned}\hat{\sigma}_v^2&=\frac{1}{(M-1)(n-p)}\sum_{t=1}^{M}(\mathbf{y}(t)-\overline{\mathbf{y}})^T(\mathbf{I}-\boldsymbol{\Gamma}\boldsymbol{\Gamma}^+)^T(\mathbf{I}-\boldsymbol{\Gamma}\boldsymbol{\Gamma}^+)(\mathbf{y}(t)-\overline{\mathbf{y}})\\&=\frac{1}{(M-1)(n-p)}\mathrm{tr}\left\{\sum_{t=1}^{M}(\mathbf{y}(t)-\overline{\mathbf{y}})^T(\mathbf{I}-\boldsymbol{\Gamma}\boldsymbol{\Gamma}^+)(\mathbf{y}(t)-\overline{\mathbf{y}})\right\}\\&=\frac{1}{(n-p)}\mathrm{tr}\left\{(\mathbf{I}-\boldsymbol{\Gamma}\boldsymbol{\Gamma}^+)\cdot\frac{1}{M-1}\sum_{t=1}^{M}(\mathbf{y}(t)-\overline{\mathbf{y}})(\mathbf{y}(t)-\overline{\mathbf{y}})^T\right\}\\&=\frac{1}{(n-p)}\cdot\mathrm{tr}((\mathbf{I}-\boldsymbol{\Gamma}\boldsymbol{\Gamma}^+)\cdot\mathbf{S}_y).\end{aligned} \tag{a6}$$

After obtaining the solution of $\hat{\sigma}_v^2$, we can substitute it into (a2) to solve for $\hat{\sigma}_i^2$ as

$$\hat{\sigma}_i^2 = \frac{1}{(\boldsymbol{\gamma}_i^T \boldsymbol{\gamma}_i)^2} \mathrm{tr}(\boldsymbol{\gamma}_i \boldsymbol{\gamma}_i^T \mathbf{S}_y) - \hat{\sigma}_v^2 \cdot \frac{1}{\boldsymbol{\gamma}_i^T \boldsymbol{\gamma}_i}, \quad i = 1,2,\ldots,p. \quad (a7)$$

Recall that $\mathrm{tr}(\boldsymbol{\gamma}_i \boldsymbol{\gamma}_i^T \mathbf{S}_y) = \boldsymbol{\gamma}_i^T \mathbf{S}_y \boldsymbol{\gamma}_i$ and $1/\boldsymbol{\gamma}_i^T \boldsymbol{\gamma}_i$ is the (i,i) element of $(\boldsymbol{\Gamma}^T \boldsymbol{\Gamma})^{-1}$. Then, $\boldsymbol{\gamma}_i^T / \boldsymbol{\gamma}_i^T \boldsymbol{\gamma}_i$ is the ith row of $(\boldsymbol{\Gamma}^T \boldsymbol{\Gamma})^{-1} \boldsymbol{\Gamma}^T$. We can further write $(a7)$ as

$$\hat{\sigma}_i^2 = \frac{\boldsymbol{\gamma}_i^T}{\boldsymbol{\gamma}_i^T \boldsymbol{\gamma}_i} \mathbf{S}_y \frac{\boldsymbol{\gamma}_i}{\boldsymbol{\gamma}_i^T \boldsymbol{\gamma}_i} - \hat{\sigma}_v^2 \cdot \frac{1}{\boldsymbol{\gamma}_i^T \boldsymbol{\gamma}_i} = \boldsymbol{\Gamma}_i^+ \mathbf{S}_y (\boldsymbol{\Gamma}_i^+)^T - \hat{\sigma}_v^2 (\boldsymbol{\Gamma}^T \boldsymbol{\Gamma})_{i,i}^{-1},$$
$$i = 1,2,\ldots,p, \quad (a8)$$

where $\boldsymbol{\Gamma}_i^+$ is the ith row of $(\boldsymbol{\Gamma}^T \boldsymbol{\Gamma})^{-1} \boldsymbol{\Gamma}^T$. The second term $\hat{\sigma}_v^2 (\boldsymbol{\Gamma}^T \boldsymbol{\Gamma})_{i,i}^{-1}$ in the right hand side of the above equation is the same as the one in (DP3) in Section 1. We shall show that $\Sigma_{t=1}^M \hat{u}_i(t)^2/(M-1)$ is the same as $\boldsymbol{\Gamma}_i^+ \mathbf{S}_y (\boldsymbol{\Gamma}_i^+)^T$. In fact, $\hat{u}_i(t) = ((\boldsymbol{\Gamma}^T \boldsymbol{\Gamma})^{-1} \boldsymbol{\Gamma}^T)_i \cdot (\mathbf{y}(t) - \overline{\mathbf{y}}) = \boldsymbol{\Gamma}_i^+ (\mathbf{y}(t) - \overline{\mathbf{y}})$. Then,

$$\frac{1}{M-1} \sum_{t=1}^{M} \hat{u}_i(t)^2 = \frac{1}{M-1} \sum_{t=1}^{M} (\boldsymbol{\Gamma}_i^+ (\mathbf{y}(t) - \overline{\mathbf{y}}))(\boldsymbol{\Gamma}_i^+ (\mathbf{y}(t) - \overline{\mathbf{y}}))^T$$
$$= \boldsymbol{\Gamma}_i^+ \cdot \left(\frac{1}{M-1} \sum_{t=1}^{M} (\mathbf{y}(t) - \overline{\mathbf{y}})(\mathbf{y}(t) - \overline{\mathbf{y}})^T \right) \cdot (\boldsymbol{\Gamma}_i^+)^T$$
$$= \boldsymbol{\Gamma}_i^+ \cdot \mathbf{S}_y \cdot (\boldsymbol{\Gamma}_i^+)^T. \quad (a9)$$

This completes the proof. ◇

References

[1] Shalon, D., Gossard, D., Ulrich, K., and Fitzpatrick, D., 1992, "Representing Geometric Variations in Complex Structural Assemblies on CAD Systems," *Proceedings of the 19th Annual ASME Advances in Design Automation Conference*, DE-Vol. 44-2, pp. 121–132.

[2] Ceglarek, D., and Shi, J., 1995, "Dimensional Variation Reduction for Automotive Body Assembly," Manufacturing Review, **8**, pp. 139–154.

[3] Cunningham, T. W., Mantripragada, R., Lee, D. J., Thornton, A. C., and Whitney D. E., 1996, "Definition, Analysis, and Planning of a Flexible Assembly Process," *Proceedings of the 1996 Japan/USA Symposium on Flexible Automation*, Vol. 2, pp. 767–778.

[4] Ceglarek, D., and Shi, J., 1996, "Fixture Failure Diagnosis for the Autobody Assembly Using Pattern Recognition," ASME J. Ind., **118**, pp. 55–66.

[5] Apley, D. W., and Shi, J., 1998, "Diagnosis of Multiple Fixture Faults in Panel Assembly," ASME J. Manuf. Sci. Eng., **120**, pp. 793–801.

[6] Chang, M., and Gossard, D. C., 1998, "Computational Method for Diagnosis of Variation-Related Assembly Problem," Int. J. Prod. Res., **36**, pp. 2985–2995.

[7] Rong, Q., Ceglarek, D., and Shi, J., 2000, "Dimensional Fault Diagnosis for Compliant Beam Structure Assemblies," ASME J. Manuf. Sci. Eng., **122**, pp. 773–780.

[8] Carlson, J. S., Lindkvist, L., and Soderberg, R., 2000, "Multi-Fixture Assembly System Diagnosis Based on Part and Subassembly Measurement Data," *Proceedings of the 2000 ASME Design Engineering Technical Conference*, September 10–13, Baltimore, MD.

[9] Ding, Y., Ceglarek, D., and Shi, J., 2002, "Fault Diagnosis of Multi-Station Manufacturing Processes by Using State Space Approach," ASME J. Manuf. Sci. Eng., **124**, pp. 313–322.

[10] Ding, Y., Shi, J., and Ceglarek, D., 2002, "Diagnosability Analysis of Multi-Station Manufacturing Processes," ASME J. Dyn. Syst., Meas., Control, **124**, pp. 1–13.

[11] Rong, Q., Shi, J., and Ceglarek, D., 2001, "Adjusted Least Squares Approach for Diagnosis of Ill-Conditioned Compliant Assemblies," ASME J. Manuf. Sci. Eng., **123**, pp. 453–461.

[12] Schott, J. R., 1997, *Matrix Analysis for Statistics*, John Wiley & Sons, New York.

[13] Golub, G. H., and Van Loan, C. F., 1996, *Matrix Computations*, 3rd ed., The Johns Hopkins University Press, Baltimore, MD.

[14] Geladi, P., and Kowalski, B. R., 1986, "Partial Least-Squares Regression: A Tutorial," Anal. Chim. Acta, **185**, pp. 1–17.

[15] Beck, J. V., and Arnold, K. J., 1977, *Parameter Estimation in Engineering and Science*, John Wiley & Sons, New York.

[16] Hasan, W. M., and Viloa, E., 1997, "Use of the Singular Value Decomposition Method to Detect Ill-Conditioning of Structural Identification Problems," Comput. Struct., **63**, pp. 267–275.

[17] Jin, J., and Shi, J., 1999, "State Space Modeling of Sheet Metal Assembly for Dimensional Control," ASME J. Manuf. Sci. Eng., **121**, pp. 756–762.

[18] Ding, Y., Ceglarek, D., and Shi, J., 2000, "Modeling and Diagnosis of Multi-Station Manufacturing Processes: Part I State Space Model," *Proceedings of the 2000 Japan/USA Symposium on Flexible Automation*, July 23–26, Ann Arbor, MI, 2000JUSFA-13146.

[19] Mantripragada, R., and Whitney, D. E., 1999, "Modeling and Controlling Variation Propagation in Mechanical Assemblies Using State Transition Models," IEEE Trans. Rob. Autom., **15**, pp. 124–140.

[20] Camelio, A. J., Hu, S. J., and Ceglarek, D. J., 2001, "Modeling Variation Propagation of Multi-Station Assembly Systems With Compliant Parts," *Proceedings of the 2001 ASME Design Engineering Technical Conferences*, September 9–12, Pittsburgh, PA.

[21] Djurdjanovic, D., and Ni, J., 2001, "Linear State Space Modeling of Dimensional Machining Errors," Transactions of NAMRI/SME, **XXIX**, pp. 541–548.

[22] Zhou, S., Huang, Q., and Shi, J., 2003, "State Space Modeling for Dimensional Monitoring of Multistage Machining Process Using Differential Motion Vector," IEEE Trans. Rob. Autom., **19**, pp. 296–308.

[23] Luenberger, D. G., 1968, *Optimization by Vector Space Methods*, Wiley, New York.

[24] Pukelsheim, F., 1993, *Optimal Design of Experiments*, John Wiley and Sons, New York.

[25] Anderson, T. W., 1973, "Asymptotic Efficient Estimation of Covariance Matrices With Linear Structure," Annals of Statistics, **1**, 135–141.

[26] Neter, J., Hutner, M. H., Nachtsheim, C. J., and Wasserman, W., 1996, *Applied Linear Statistical Models*, 4th ed., McGraw Hill-Irwin, Chicago, IL.

[27] Rao, C. R., and Kleffe, J., 1988, *Estimation of Variance Components and Applications*, North-Holland, Amsterdam, p. 225.